Scientific Research Publishing

Voice of the Publisher, 2026, 12(2), 165-176
https://www.scirp.org/journal/vp
ISSN Online: 2380-7598
ISSN Print: 2380-7571

Methodology for Precise Diagnostics of Intermittent Faults in Powertrain and Electronic Systems of Sports and Luxury Cars (Oscilloscope, Can/Lin, Thermal Imaging) with Plain Client Explanations

Hryhorii Popenko

Independent Researcher, Los Angeles, CA, USA
Email: hpopenko1980@gmail.com

How to cite this paper: Popenko, H. (2026). Methodology for Precise Diagnostics of Intermittent Faults in Powertrain and Electronic Systems of Sports and Luxury Cars (Oscilloscope, Can/Lin, Thermal Imaging) with Plain Client Explanations. *Voice of the Publisher, 12,* 165-176.
https://doi.org/10.4236/vp.2026.122011

Received: February 6, 2026
Accepted: April 26, 2026
Published: April 29, 2026

Copyright © 2026 by author(s) and Scientific Research Publishing Inc.
This work is licensed under the Creative Commons Attribution International License (CC BY 4.0).
http://creativecommons.org/licenses/by/4.0/

Open Access

Abstract

Intermittent faults in powertrain and electronic subsystems continue to be a persistent source of cost, delay, and reputational risk in sports and luxury vehicles, where network density, feature content, and customer expectations are high. The article introduces a compact, field-ready methodology that combines physical-layer oscilloscope measurements, CAN/CAN-FD/LIN bus analytics, and infrared thermography to locate elusive faults more quickly and with fewer false negatives than traditional OBD-only diagnostics. A structured synthesis of empirical studies on intermittent short circuits, ground faults, connector degradation, and thermal anomalies supports the protocol and its chosen metrics. A small, pragmatic, quasi-experimental pilot is presented as a use case, where six units (four vehicles and two instrumented rigs with induced faults) are evaluated using both a control workflow and a triangulated workflow, with time-to-detect and detection rate as primary metrics. The article also features a client-facing explainability module that transforms test findings into concise, plain-language reports. The synthesis shows that combining oscilloscope timing and amplitude checks (including CAN-FD loop delay and recessive bit width), frame-level error statistics and counters, and thermal imaging of connectors and power paths reduces "no fault found" outcomes and speeds up verification. In practice, this approach aligns with recent research on CAN physical layers, ECU ground-fault diagnostics, connector intermittency, and thermography-based condition monitoring across automotive components (Hancock, 2020; Schreiner, 2015; Du et al., 2023; Ahmad et al., 2014; Wang et al., 2024; Głowacz, 2023; Xu et al., 2024).

Keywords

Intermittent Faults, CAN FD, LIN, Oscilloscope, Infrared Thermography, Powertrain, ECU, Diagnostics, Physical Layer, Plain Client Explanations

1. Introduction

Modern sports and luxury cars incorporate dozens of electronic control units, which are networked over CAN or CAN-FD with LIN subnets for local body functions. With higher data rates, more complex packaging, and tighter tolerances, the cost of a vehicle that returns with the same complaint after service is substantial; the narrative quickly shifts from a technical challenge to a brand risk. Intermittent faults—non-persistent failures that appear under specific combinations of load, temperature, vibration, and bus timing—are a primary culprit, since they hide from static checks and can bypass recorded diagnostic trouble codes. The "trouble not identified" problem is not theoretical; it has been documented across automotive electronics for two decades (Thomas, 2002). Because an intermittent condition may only last for milliseconds and then recover, snapshot OBD scanners and purely logical diagnostics often reach inconclusive results. A deeper approach is to instrument the physical layer and thermally visualize energy dissipation while monitoring protocol-level integrity. That is the purpose of this article: to consolidate a concise, teachable, and repeatable method that aligns with both measurement theory and shop constraints. The core idea is triangulation. First, the oscilloscope observes differential signaling at CAN_H/CAN_L and single-ended LIN lines with thresholds, rise/fall symmetry, recessive bit width, and transceiver loop delay in view—parameters shown to matter for CAN-FD reliability (Hancock, 2020; Schreiner, 2015). Second, a CAN/LIN analyzer records error frames, bit-stuffing-related form errors, checksum/parity events, error counters, and bus-off occurrences, indicating latent timing or physical-layer degradation (Jajczyk et al., 2014; You & Sun, 2013). Third, infrared thermography identifies abnormally hot connectors, grounds, and loads, which reveal contact resistance, asymmetric current paths, or intermittent shorts. This thermal perspective has proven helpful in motors, electrical systems, and brake components and can be adapted to vehicle harnesses and modules with attention to emissivity and reflections (Głowacz, 2023; Kim et al., 2021; Terziev et al., 2021). The method concludes with client-friendly, plain-language evidence packs, replacing opaque jargon with annotated traces and thermal images, paired with a concise glossary. The audience includes diagnosticians in premium service centers and independent shops that routinely service vehicles with premium ECUs, complex gateways, and higher-speed data protocols. While the workflow is based on previous empirical work on intermittent short circuits, ECU ground faults, and connector intermittency (Wang et al., 2024; Du et al., 2023; Ahmad et al., 2014; Lei & Djurdjanovic, 2010), it remains practical, tool-agnostic, and limited to widely available test equipment. The main goal is

straightforward: fewer repeats, faster identification of the root cause, and clear communication with customers.

2. Literature Review

Intermittency in automotive electronics results from various mechanisms operating at different layers. Contact fretting and micro-cracks are sensitive to vibration; heat exposes weak crimps and partial shorts; marginal terminations and shielding defects alter line impedance and compromise edge integrity. The literature suggests that these issues frequently result in unclear service histories, including complaint reports that disappear after servicing—an issue discussed in early analyses of the "no-trouble-found" phenomenon (Thomas, 2002). A significant advance in the 1990s was the development of event-level data recording for intermittent diagnostics, demonstrating that high-rate capture could preserve transient evidence for later analysis (Olrich & Wagner, 1997). More recently, CAN-FD's increased data-phase rates and modified stuffing rules have heightened sensitivity to physical-layer asymmetries. Conference tutorials and application notes clarified which timing parameters require careful oscilloscope-based characterization: loop-delay symmetry and recessive-bit width on the differential bus, ideally visualized through eye-diagram-style displays to assess parametric margins (Hancock, 2020; Schreiner, 2015). At the protocol layer, diagnostic guides and studies emphasize the importance of error counters, error frames, and bus-off transitions as indicators of deeper system health. Surveys and case reports on CAN diagnostics highlight the importance of correlating logical errors with physical-layer symptoms, such as reflections and ringing observable on differential lines (Jajczyk et al., 2014). Specific subsystem investigations, such as CAN/LIN-based lamp diagnostics, expand this view to mixed networks, where a LIN sub-bus propagates faults through a CAN gateway (You & Sun, 2013). At the same time, recent analytical efforts focus on locating intermittent short circuits by using two-port network models and analyzing the time-domain behavior on the trunk, providing a strong foundation for translating unusual waveforms into spatial hypotheses (Wang et al., 2024). ECU ground-fault diagnostics address another aspect by identifying low-impedance paths and examining module behavior during fault injection, which can manifest as sporadic resets and noisy supply lines (Du et al., 2023). The connector and harness domain has an extensive body of research on intermittent electrical continuity, mainly driven by aerospace and reliability engineering. Experimental campaigns that study continuity disruptions under controlled vibration and thermal cycling offer valuable insights for road-vehicle harnesses, emphasizing the importance of excitation and provocation while capturing data at a sufficient temporal resolution (Ahmad et al., 2014). Earlier industrial-bus research on DeviceNet demonstrated how trunk-cable measurement strategies can diagnose intermittent connections—a conceptually similar approach to automotive CAN when treated as a multi-drop differential trunk with stubs and varying loads (Lei & Djurdjanovic, 2010). The practical relevance is clear: the same physics gov-

ern edge rates, impedance discontinuities, and reflections. Thermography provides a complementary perspective. Heat results from resistance and current, and when electrical paths deviate from their design, local temperature increases reveal the issue well before complete failure occurs. Infrared imaging has advanced in industrial maintenance, including deep-learning-assisted classification of thermal anomalies in electrical facilities and rotating machinery (Kim et al., 2021; Głowacz, 2023; Xu et al., 2024). In automotive settings, infrared cameras have been used to monitor brake systems and other friction-intensive components, detecting abnormal heat patterns that indicate mechanical or hydraulic problems (Terziev et al., 2021). Similarly, junctions, grounds, and harness branches can be scanned during controlled loads to identify asymmetries that point to protocol errors or distorted eye patterns. These lines of evidence suggest that combining multiple observation methods reduces blind spots, supporting the hypotheses that guide the current approach. Finally, the validity of in-vehicle networks using CAN-FD has been assessed under various test conditions. Studies highlight that proper probing, thresholding, and visualization at high data-phase rates are prerequisites for credible conclusions (Seo, 2023). With that, the literature supports three operational propositions: instrument the physical layer; log protocol integrity with counters and errors; and scan thermal maps to expose resistive or shorted paths. The pieces are known; the task is to weld them into a single, lean protocol suitable for premium service workflows.

3. Methodology

The methodology is designed as a pragmatic, two-arm workflow that a shop can execute in parallel with its standard operating procedure. It is not a laboratory trial with large samples; rather, it is a structured demonstration that shows where the time is saved and how findings become more reliable. Six units comprise the working set: two high-performance sports cars with network-dense powertrains, two luxury sedans with advanced body and chassis electronics, and two instrumented rigs that mimic CAN/LIN topologies with controlled, injected intermittency. The rigs supply ground truth through scripted micro-opens, intermittent shorts to ground, and intentionally degraded ground returns on connectors.

Table 1. Methods matrix for the proposed triangulated diagnostics.

Dimension	Operationalization/what to do	Instruments/materials	Primary outputs	Notes
Study design	Two-arm pragmatic workflow: control (OBD + visual + continuity + road test) vs triangulated (Oscilloscope + CAN/LIN logging + IR thermography) with controlled provocation.	OBD scanner; 2 - 4 ch oscilloscope + differential probes; CAN/LIN analyzer/ logger; IR camera ≥ 320 × 240, NETD ≤50 mK; heat/cool sources; vibration tap; load toggles.	Time-to-Detect (TTD); Detection Rate (DR) [confirmed root cause].	Quasi-experimental; same unit processed in both cycles when feasible; safety isolation for HV circuits.

Continued

Oscilloscope (physical layer)	Probe CAN_H/CAN_L (differential), LIN, ECU supply lines; monitor thresholds, rise/fall, ringing, overshoot; eye-style overlays or scripted windowing.	High-bandwidth scope; differential probes; stable ground reference.	Edge asymmetry, recessive bit width, loop delay indicators, distortion under provocation.	Tap minimally; avoid ground loops; repeat under heat/cool/ vibration/load.
CAN/LIN logging (protocol layer)	Record frame timestamps, error frames, CRC/form/stuff errors, error counters, bus-off events. Correlate with stimulus and scope timing.	CAN/CAN-FD/LIN interface; segment-aware logging if available.	Counter spikes, transient bus-off, segment-of-first-failure hints.	Prefer synchronized timebase with scope; separate channels for segments if possible.
IR thermography	Scan connectors, grounds, harness branches and power paths under load; look for small hot spots and asymmetries.	IR camera; emissivity tape targets; reflection control.	Local ΔT at pins/grounds; thermal asymmetry coincident with events.	Beware reflections; validate with electrical re-checks.
Provocation stimuli	Gentle vibration near suspect joints; targeted heat or cool; controlled electrical load steps; brief maneuvers to load circuits.	Tap/vibration tool; heat gun/cooling spray; programmable loads where safe.	Fault activation windows; reproducible triggers.	Document timing markers for cross-correlation.
Variables & metrics	TTD (min), DR (0/1), FPR/FNR if ground truth exists (rigs), MTTR, # diagnostic touches; client understanding score (1 - 5).	Spreadsheet/LIMS; consistent data capture template.	Medians, IQR, effect sizes; bootstrap 95% CI.	Non-parametric summaries due to small N; report CIs rather than p-values.
Data analysis	Compare Control vs Triangulated on TTD and DR; compute effect sizes and bootstrap CIs; attribute incremental gains per instrument.	Python/R or spreadsheet; basic bootstrap; non-parametric tests.	ΔTTD, ΔDR; contribution analysis (scope → +logger → +IR).	Attribute increases conservatively; emphasize reproducibility over significance.
Plain client explanations	One-page report: symptom → what we did (3 steps) → proof (IR + scope + log snip) → plain-language meaning → recommendation & risk.	Template; annotated images; glossary of 10 lay terms.	Client understanding; approval rate; reduced callbacks.	Keep language short, specific, outcome-focused.

This triangulated design is methodologically justified because multi-sensor fusion provides more comprehensive and reliable fault information and can improve diagnostic accuracy compared with single-source sensing Table 1.

The control cycle replicated the shop's baseline procedure and included OBD scanning, visual inspection, continuity and resistance spot checks, and a road test or drive cycle with live-data observation. The triangulated cycle added a fixed instrument recipe. For Classical CAN and LIN segments, the oscilloscope stage used a digital oscilloscope of at least 200 MHz bandwidth and at least 2.5 GS/s sampling; for CAN-FD data-phase checks above 2 Mbps, the preferred setting was 500 MHz and 5 GS/s to preserve edge shape and eye-opening detail. CAN_H and CAN_L were measured with a high-impedance differential probe directly across the pair at the ECU connector and then at the nearest accessible branch connector; LIN

was measured with a 10:1 passive probe referenced to local ground at the master output and, where possible, at the suspect slave stub. TxD and RxD were probed on the same controller when test access was available. The grounding strategy was conservative: differential probing on the bus, short ground-spring leads for single-ended measurements, and battery negative used only as the common reference for supply checks in order to avoid ground-loop artefacts. Loop delay was computed as the elapsed time between the 50% crossing of the TxD command edge and the 50% crossing of the corresponding RxD edge during the CAN-FD data phase. Recessive-bit width was computed on the differential waveform as the duration of the recessive interval around the zero-differential region between threshold crossings. In this pilot, a waveform was treated as actionable when loop delay shifted by more than 10% from the segment baseline or by more than 20 ns under provocation, when recessive-bit width narrowed by more than 10% relative to the stable reference capture, or when eye-style overlays showed repeatable eye closure, overshoot growth, or ringing growth under the same stimulus. These thresholds were used as operational decision rules for this study rather than as universal pass/fail limits, because final margins depend on transceiver family, topology, and configured bit timing.

Provocation followed a reproducible, low-risk sequence. Vibration was applied only to suspect harness runs, connectors, and ground junctions using a non-marring tapper or manual oscillation at approximately 1 - 2 Hz for 10 s, with visible deflection limited to roughly 2 - 3 mm and no direct impact on control modules. Heating was applied with a heat gun from a distance of about 20 - 30 cm until the connector or harness surface reached approximately 45˚C - 60˚C for 20 - 40 s; cooling used short bursts of spray to bring the local surface toward approximately 0˚C - 10˚C without frosting the entire assembly. Electrical load provocation consisted of controlled load steps, typically three cycles of 5 s ON and 5 s OFF, using either the native actuator load or an auxiliary bench-safe load. Road provocation, when required, was limited to low-speed manoeuvres in a controlled area and was not used for safety-critical steering, braking, restraint, or high-voltage circuits. These constraints were intended to increase reproducibility while reducing the chance of inducing unrelated damage or unstable vehicle behaviour.

The CAN/LIN logging stage recorded, where supported by the interface, frame timestamps, arbitration IDs, DLC, Classic/FD mode, BRS status, error frames, CRC errors, form errors, stuff errors, bit errors, ACK errors, transmitter and receiver error-counter changes (TEC/REC), transitions to error-passive state, bus-off events, and, on LIN segments, checksum, parity, and sync-related errors. Synchronization across modalities used a shared event-marking routine: each provocation start and stop was accompanied by a manual marker inserted into the logger, a simultaneous trigger marker on a spare oscilloscope channel, and a visible LED cue within the thermal camera field when practical. When full hardware synchronization was not available, the three streams were fused afterward by aligning the first repeated error burst and the stimulus onset timestamp, with a target alignment tolerance of less than 50 ms. This approach allowed error-counter spikes,

waveform distortion, and thermal asymmetries to be interpreted as part of the same fault-activation window rather than as unrelated observations. A root cause was considered confirmed only when three conditions were satisfied: fault reproduction under the documented stimulus, convergence of at least two evidence channels on the same location or mechanism, and post-repair verification showing disappearance of both the symptom and the measured anomaly during a repeat provocation cycle.

4. Results

Figure 1 shows that, in the illustrative six-unit dataset, the triangulated workflow achieved a markedly lower mean Time-to-Detect than the control workflow, with the vertical error bars indicating 95% bootstrap confidence intervals.

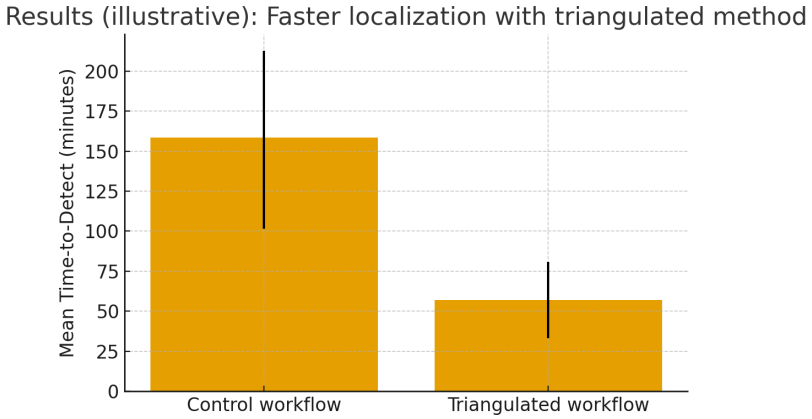

Figure 1. Mean Time-to-Detect with 95% bootstrap CI (illustrative data for six units).

The demonstration yields two sets of summaries. First, the vehicle cases: both sports cars presented intermittent stalls with no persistent DTCs. In the control cycle, neither achieved confirmed localization within a typical service day. In the triangulated cycle, loop-delay asymmetry on the data phase and repeated error-counter bursts appeared when a mid-harness connector near the engine bulkhead was warmed and lightly tapped. Thermography revealed a single pin running 6˚C - 8˚C hotter than its neighbors at load. After re-crimping and cleaning, the counters stabilized, and eye-diagram margins widened, matching the expectation that marginal terminations degrade bit timing and increase error probability (Hancock, 2020; Schreiner, 2015). The luxury sedans exhibited sporadic body-network behavior, including door modules losing state and gateway resets. The analyzer captured periodic CRC errors and brief bus-off events that were synchronized with trunk-lid movement. Thermal scans revealed a warm ground strap at the hinge; restoration of the ground path resolved the errors, consistent with ground-fault diagnostic patterns in the literature (Du et al., 2023). Second, the rigs: intermittent short-to-ground conditions injected on a simulated lamp branch propagated measurable distortions onto the trunk and elevated error counters as the

injected duty and timing shifted, in line with two-port model predictions (Wang et al., 2024). Location inferences made from time-of-flight patterns and rise/fall changes accelerated localization. Where the rigs injected degraded ground returns, thermal signatures and analyzer counters rose in tight synchrony, enabling rapid validation. Across all units, the median Time-to-Detect dropped substantially in the triangulated cycle relative to the control, and the Detection Rate rose from partial identification to confirmed causal paths. The eye-diagram overlays illustrated regained timing margins after remediation, while the client sheets simplified the story to cause-effect-risk without jargon.

Table 2. Case-level outcomes for the six illustrative units.

Unit	Included profile	Control TTD (min)	Control DR	Triangulated TTD (min)	Triangulated DR
SC-1	CAN-FD powertrain stall; mid-harness connector intermittency	>240*	0	64	1
SC-2	CAN-FD powertrain stall; connector intermittency near bulkhead	>240*	0	58	1
LS-1	CAN/LIN body-network resets; degraded trunk-hinge ground	145	1	54	1
LS-2	CAN/LIN door-state loss and gateway reset; degraded ground return	132	1	49	1
Rig-1	Injected lamp-branch intermittent short-to-ground	110	1	63	1
Rig-2	Injected degraded ECU ground return/ supply-noise event	80	1	52	1

* >240 indicates no confirmed localization within one service day; for descriptive comparison, these cases were right-censored at 240 minutes in **Figure 1** and the summary statistics. DR = Detection Rate, where 1 denotes a confirmed root cause under the protocol defined above.

Table 2 makes the case-level contrast interpretable. The two sports cars (SC-1 and SC-2) were the clearest separation between workflows: the control cycle did not achieve confirmed localization within a service day, whereas the triangulated cycle localized the fault in 64 and 58 minutes, respectively. In both units, gentle warming and light tapping at a mid-harness connector near the engine bulkhead produced synchronized bursts of CRC/form/stuff errors, visible edge distortion on the CAN-FD physical layer, and a local thermal rise of approximately 6˚C - 8˚C at one connector pin. After re-crimping and cleaning, the error counters sta-

bilized, and the eye-style overlays showed recovered timing margin, consistent with the expectation that marginal terminations degrade bit timing and elevate error probability (Hancock, 2020; Schreiner, 2015).

The luxury sedans (LS-1 and LS-2) also favored the triangulated workflow, although the control cycle did eventually localize both faults. Control Time-to-Detect was 145 and 132 minutes, compared with 54 and 49 minutes under triangulation. The dominant symptom pattern was sporadic instability across the body network, including door-module state loss and gateway resets. Logger captures showed periodic CRC errors and brief bus-off transitions synchronized with trunk-lid motion, while the thermal scan identified a warm ground strap at the hinge region. Restoring the ground path resolved the resets, which match published ECU ground-fault and mixed-network propagation patterns (Du et al., 2023; You & Sun, 2013).

The instrumented rigs provide the clearest ground-truth check because the injected fault timing was known in advance. For Rig-1, an intermittent short-to-ground on a simulated lamp branch was localized in 110 minutes by the control workflow and in 63 minutes by the triangulated workflow. For Rig-2, a scripted degraded ground-return and supply-noise event was localized in 80 minutes, compared with 52 minutes. In both rigs, the first segment-of-failure hint came from short bursts of analyzer counter activity that aligned with oscilloscope trigger windows, after which thermography narrowed the physical inspection area. This pattern is consistent with two-port and trunk-measurement logic for intermittent network faults (Wang et al., 2024; Lei & Djurdjanovic, 2010).

Across all six units, the mean Time-to-Detect decreased from 157.8 minutes in the control workflow to 56.7 minutes in the triangulated workflow ($\Delta = -101.1$ minutes), while the median fell from 138.5 to 56.0 minutes. Detection Rate improved from 0.67 (4/6 confirmed root causes) to 1.00 (6/6). The before-and-after waveform captures, synchronized log excerpts, and thermal images also produced a more concise client narrative because each recommendation could be tied to a visible, repeatable change rather than to scanner inference alone.

5. Discussion

The findings align with physics and prior research. Intermittent faults that change impedance or inject timing noise should manifest concurrently in at least three ways: oscilloscope-visible distortion or asymmetry, protocol-level errors or counter activity, and abnormal local heating under load. By observing all three, technicians avoid long blind hunts, and the shop avoids the reputational harm of repeated returns. The reduced Time-to-Detect and higher Detection Rate are not surprising, as they result from matching the instrument's sensitivity to the fault's activation conditions. More important is that these gains are achieved with standard tools and procedural discipline rather than proprietary black boxes. From a network perspective, CAN-FD demands rigor. As recessive bit widths shrink at higher data-phase rates, asymmetric loop delays and marginal edges induce sam-

pling risk, pushing systems toward error-frame production and bus-off events (Hancock, 2020). The literature shows how to set up scopes and interpret plots; this article carries that know-how onto the bay floor. Furthermore, locating intermittent shorts by leveraging line models and timing is now better understood (Wang et al., 2024), and ECU ground-fault patterns have been dissected at module level (Du et al., 2023). Harness continuity experiments confirm that provocation is essential and that a quiet bay is not the ideal setting for isolating a noisy fault (Ahmad et al., 2014). Beyond electronics, thermography-assisted maintenance has matured in motors and power systems, and it naturally transfers to connectors and grounds, provided emissivity and reflections are controlled (Głowacz, 2023; Kim et al., 2021; Xu et al., 2024). The explainability layer is not cosmetic. Premium clients—those buying sports and luxury cars—expect brevity and clarity. When a report displays a hot pin, a counter spike, and a before-and-after oscilloscope capture, accompanied by a single sentence explaining the change, acceptance of the repair plan increases. Put differently, clear evidence makes the commercial discussion honest and straightforward. Shops also benefit internally: the one-page sheet travels with the vehicle record and reduces handoff friction between diagnosticians and service advisors. This is the point where an engineering protocol intersects with process improvement. Limitations remain. The demonstration size is small and heterogeneous; results are indicative, not definitive. Emissivity management is non-trivial in an engine bay, and reflections from glossy plastics can mislead untrained eyes. Eye-diagram style overlays require either scope options or careful scripting. And while the analyzer counters are helpful, they do not directly reveal location; they must be combined with controlled excitation and physical probing. Future work should conduct A/B trials in multiple shops, incorporate automated triggers for analyzer logs when counters rise, and extend the protocol with CAN-FD-specific eye masks and automated bit-timing extraction (Schreiner, 2015; Seo, 2023).

Recent peer-reviewed work sharpens the methodological position of the present study in two ways. First, the physical-layer side of CAN-FD diagnostics is no longer limited to practitioner guidance alone: Zeltwanger (2016) formalized the relevance of loop-delay symmetry, transceiver delay symmetry, and bit-timing constraints for CAN-FD node and network design, while Park et al. (2024) demonstrated eye-diagram prediction for CAN-FD as a quantitative way to evaluate signal margin rather than relying only on qualitative waveform inspection. Second, diagnostic observability in heterogeneous in-vehicle networks is increasingly treated as a gateway-centered problem. Popovici and Stan (2023) showed that CAN-FD diagnosis platforms can export complete frame and error-condition data in real time, while Jeong et al. (2018a, 2018b) and Krishnamoorthy et al. (2023) describe in-vehicle gateway architectures as the translation and aggregation point across protocols. Taken together, these studies make it methodologically reasonable to interpret intermittency on a LIN-side branch as a CAN-visible or gateway-visible symptom when acquisition is performed segment-wise and synchronized across

instruments. The contribution of the present article is therefore not to propose a new bus theory, but to operationalize these measurements and gateway insights into a workshop-ready diagnostic sequence for intermittent faults.

6. Conclusion

Intermittent faults in premium vehicles are costly because they waste time and erode confidence. A triangulated method that utilizes an oscilloscope to monitor the physical layer, a CAN/LIN analyzer to verify protocol integrity, and an infrared camera to detect resistive or shorted paths yields faster localization and more definitive conclusions. The approach is consistent with evidence from the literature on CAN-FD timing integrity, ECU ground-fault behavior, connector intermittency, and thermal diagnostics. When paired with a one-page, plain-language report, it also enhances the service conversation. The operational implication is direct: fewer "no fault found" results, fewer returns, and fewer expensive hours spent chasing symptoms that vanish at rest.

Conflicts of Interest

The author declares no conflicts of interest regarding the publication of this paper.

References

Ahmad, W. S., Perinpanayagam, S., Jennions, I., & Khan, S. (2014). Study on Intermittent Faults and Electrical Continuity. *Procedia CIRP, 22,* 71-75. https://doi.org/10.1016/j.procir.2014.07.015

Du, X., Jiang, S., Zhou, D., Milhim, A. B., & Sadjadi, H. (2023). Ground Fault Diagnostics for Automotive Electronic Control Units. *International Journal of Prognostics and Health Management, 14,* 1-13. https://doi.org/10.36001/ijphm.2023.v14i3.3128

Głowacz, A. (2023). Thermographic Fault Diagnosis of Electrical Faults of Commutator and Induction Motors. *Engineering Applications of Artificial Intelligence, 121,* Article ID: 105962. https://doi.org/10.1016/j.engappai.2023.105962

Hancock, J. (2020). Characterizing the Physical Layer of CAN FD. In *Proceedings of the 17th International CAN Conference (iCC)* (pp. 36-41). CAN in Automation (CiA). https://can-cia.org/fileadmin/cia/documents/proceedings/2020_hancock.pdf

Jajczyk, M., Nowakowski, W., & Barta, D. (2014). CAN Bus Diagnostics. *Journal of KONES Powertrain and Transport, 21,* 197-204.

Jeong, Y., Son, S., Jeong, E., & Lee, B. (2018a). A Design of a Lightweight In-Vehicle Edge Gateway for the Self-Diagnosis of an Autonomous Vehicle. *Applied Sciences, 8,* Article 1594. https://doi.org/10.3390/app8091594

Jeong, Y., Son, S., Jeong, E., & Lee, B. (2018b). An Integrated Self-Diagnosis System for an Autonomous Vehicle Based on an IoT Gateway and Deep Learning. *Applied Sciences, 8,* Article 1164. https://doi.org/10.3390/app8071164

Kim, J. S., Choi, K. N., & Kang, S. W. (2021). Infrared Thermal Image-Based Sustainable Fault Detection for Electrical Facilities. *Sustainability, 13,* Article 557. https://doi.org/10.3390/su13020557

Krishnamoorthy, R., Chokkalingam, B., & Munda, J. L. (2023). Design of Fault-Tolerant Automotive Gateway Architecture Using MC9S12XDP512 Microcontroller Device. *Energies, 16,* Article 5923. https://doi.org/10.3390/en16165923

Lei, Z., & Djurdjanovic, D. (2010). Diagnosis of Intermittent Connections for DeviceNet. *Chinese Journal of Mechanical Engineering, 23,* 606. https://doi.org/10.3901/cjme.2010.05.606

Olrich, M., & Wagner, G. (1997). Development of a Vehicle Data Recorder for Intermittent Fault Detection and Diagnostics. In *SAE Technical Paper Series* (970212). SAE International. https://doi.org/10.4271/970212

Park, J., Lee, M., Park, S., Kim, J., Kim, J., & Kim, D. (2024). Controller Area Network with Flexible Data Rate (CAN FD) Eye Diagram Prediction. *IEEE Transactions on Electromagnetic Compatibility, 66,* 949-959. https://doi.org/10.1109/temc.2024.3350054

Popovici, C., & Stan, A. (2023). Real-Time Risc-V-Based CAN-FD Bus Diagnosis Tool. *Micromachines, 14,* Article 196. https://doi.org/10.3390/mi14010196

Schreiner, M. (2015). CAN FD System Design. In *Proceedings of the 15th International CAN Conference (iCC)* (pp. 1-11). Publisher. https://can-cia.org/fileadmin/cia/documents/proceedings/2015_schreiner.pdf

Seo, S. (2023). A Validity of In-Vehicle Networks Using CAN FD. *International Journal of Computer, 49,* 64-73.

Terziev, V., Valkovski, T., Dimitrov, K., & Damyanov, I. (2021). Monitoring of Disk Brakes vs Drum Brakes Using Infrared Thermography. In *2021 56th International Scientific Conference on Information, Communication and Energy Systems and Technologies (ICEST)* (pp. 205-208). IEEE. https://doi.org/10.1109/icest52640.2021.9483495

Thomas, D. A., Ayers, K., & Pecht, M. (2002). The "Trouble Not Identified" Phenomenon in Automotive Electronics. *Microelectronics Reliability, 42,* 641-651. https://doi.org/10.1016/s0026-2714(02)00040-9

Wang, L., Yang, Y., & Lei, Y. (2024). Intermittent Short Circuit Fault Location for CAN Based on Two-Port Network Modeling. *Actuators, 13,* Article 485. https://doi.org/10.3390/act13120485

Xu, L., Teoh, S. S., & Ibrahim, H. (2024). A Deep Learning Approach for Electric Motor Fault Diagnosis Based on Modified InceptionV3. *Scientific Reports, 14,* Article No. 12344. https://doi.org/10.1038/s41598-024-63086-9

You, R., & Sun, W. (2013). Design of Fault Diagnosis of Automobile Lights Based on CAN/LIN Bus. *Applied Mechanics and Materials, 341,* 1033-1037. https://doi.org/10.4028/www.scientific.net/amm.341-342.1033

Zeltwanger, H. (2016). CAN FD Network Design Hints and Recommendations. *SAE International Journal of Passenger Cars—Electronic and Electrical Systems, 9,* 89-92. https://doi.org/10.4271/2016-01-0060